N-Alkylated aminopyrazines for use as hydrophilic optical agents

Amruta R. Poreddy,* Bethel Asmelash, Karen P. Galen, Richard M. Fitch, Jeng-Jong Shieh, James M. Wilcox, Tasha M. Schoenstein, Jolette K. Wojdyla, Kimberly R. Gaston, John N. Freskos, William L. Neumann, Raghavan Rajagopalan, Hyo-Yang Ahn,† James G. Kostelc, Martin P. Debreczeny, Kevin D. Belfield,† and Richard B. Dorshow

Covidien Imaging Solutions, 675 McDonnell Boulevard, Hazelwood, Missouri 63042, USA

†Department of Chemistry, University of Central Florida, 4000 Central Florida Boulevard, Orlando, Florida, USA

ABSTRACT

Rapid assessment of glomerular filtration rate (GFR), which measures the amount of plasma filtered through the kidney within a given time, would greatly facilitate monitoring of renal function for patients at the bedside in the clinic. In our pursuit to develop exogenous fluorescent tracers for real-time monitoring of renal function by optical methods, N-alkylated aminopyrazine dyes and their hydrophilic conjugates based on poly (ethylene glycol) (PEG) were synthesized via reductive amination as the key step. Photophysical properties indicated a bathochromic shift on the order of 50 nm in both absorption and emission compared to naked aminopyrazines which could be very useful in enhancing both tissue penetration as well as easier detection methods. Structure–activity relationship (SAR) and pharmacokinetic (PK) studies, and the correlation of *in vivo* optical data with plasma PK for measurement of clearance (and hence GFR) are focus of the current investigation.

Keywords: GFR, renal function, PEG, pyrazine, fluorescence, reductive amination, optical monitoring, renal clearnce.

1. INTRODUCTION

Renal function is typically assessed by measuring the glomerular filtration rate (GFR) in the clinical setting. GFR measures the amount of plasma filtered through the kidney within a given time. Chronic decreases in GFR are indicative of increased cardiovascular events and increased end stage kidney failure. Acute changes in GFR are a measure of a renal insult, usually from drug toxicities, which can lead to irreversible damage if not rapidly diagnosed. The most common method of assessing renal function in the clinic involves measurement of concentration (which has an inverse relationship to GFR) of an endogenous blood marker such as serum creatinine at frequent intervals over a 24 h period.[1,2] Serum creatinine measurement has many limitations as a kidney function test since it is affected by age, state of hydration, renal perfusion, muscle mass, dietary intake, and many other anthropometric and clinical variables. The low molecular weight protein cystatin C (cysC) has been introduced as an alternative to serum creatinine for estimation of GFR.[3] However, there is no evidence to suggest that cysC is any better than serum creatinine. A series of creatinine-based GFR-estimating equations, recently extended to cysC, which take into account gender, race, and other factors, have been developed to circumvent some of the limitations of these endogenous markers.[4,5]

The availability of a rapid, dynamic (i.e. continuous, real-time), and accurate measure of renal excretion rate using exogenous markers would represent a substantial improvement over current practices. It would also be desirable to provide a method that depends solely on the renal elimination of an exogenous chemical entity so that the measurement requires less subjective interpretation based upon age, muscle mass, blood pressure, etc. Exogenous markers such as inulin,[6] iothalamate,[7] Gd-DTPA,[8] ^{99m}Tc-DTPA[9] have been developed to determine GFR, and among these, inulin is regarded as the "gold standard" for GFR measurement. Unfortunately, these markers suffer from drawbacks such as the use of ionizing radiation and laborious ex-vivo handling of blood and urine samples. Considerable effort is now being directed at developing exogenous GFR agents for rapid real-time assessment of renal function using non-radioactive methods.[10–13]

*Corresponding author. Tel.: 314 654 8328; Fax: 314 654 8900; E-mail: amruta.poreddy@covidien.com

Reporters, Markers, Dyes, Nanoparticles, and Molecular Probes for Biomedical Applications
edited by Samuel Achilefu, Ramesh Raghavachari, Proc. of SPIE Vol. 7190, 71900P
 · doi: 10.1117/12.809287

In continuation with our efforts to develop exogenous fluorescent GFR markers that absorb and emit in the visible region, we have identified simple derivatives of 2,5-diaminopyrazine-3,6-dicarboxylic acid (**1**) as low molecular weight scaffold systems with surprisingly bright emission in the yellow-to-red region of the electromagnetic spectrum.[14] A wide variety of hydrophilic pyrazine dyes that include poly (ethylene glycol) (PEG)-functionalized analogs **2** with various linkage motifs have been developed as new optical tracer molecules that function as GFR agents (Chart 1).[15] These new conjugates retain the photophysical properties of the parent pyrazine system (**1**, λ_{ex} = 406 nm, λ_{em} = 536 nm, Stokes' shift = 130 nm)[14] with typical absorption and emission maxima around 450 nm and 560 nm respectively. The dyes that would absorb and emit at longer wavelengths should further enhance the optical detection method due to their enhanced tissue penetration resulting from the minimal absorption from hemoglobin, water, and lipids.[16] Consequently, an efficient proprietary method was developed for the synthesis of *N,N'*-dialkyl pyrazines and their hydrophilic PEG-conjugates via a reductive amination route. As expected batochromic shifts on the order of ~50 nm were observed for both emission and excitation, and in this paper, renal clearance properties of this class of compounds and their structure–activity relationship (SAR) studies will be presented.

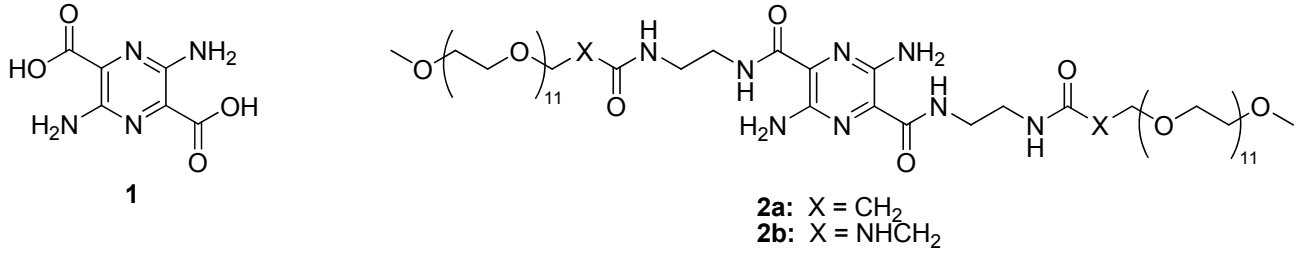

Chart 1. Low molecular pyrazine scaffold and its hydrophilic conjugates.

2. MATERIALS AND METHODS

2.1. Chemistry

Alkyl-substitution on the amino groups of pyrazine **1**[17] was shown to significantly enhance the absorption and emission maxima.[14,18,19] Esterification of the carboxylic groups of **1** with alkyl/arylalkyl halides in the presence of 1,8-diazabicyclo[5.4.0]undec-7-ene (DBU) in either *N,N*-dimethylformamide (DMF) or *N,N*-dimethylacetamide (DMAC) at ambient temperature has been reported to give variable yields (50% average) of the diester **3** (Scheme 1).[14,18] Further treatment of **3** with alkyl/arylalkyl halides at elevated temperatures (70–120 °C) gave rather low yields of *N,N'*-dalkylpyrazines **4** (3–14%). Exhaustive alkylation of **1** with alkyl/arylalkyl halides in DBU/DMAC at 70–120 °C was also found to be poor with 7–28% overall yield of **4**.[18] In an effort to improve the *N,N'*-dialkylation of pyrazine amines, reductive amination route was explored.[20] Diethyl ester **3** (R = Et), prepared in 68% yield from **1**, was reacted with 4 equiv of benzaldehyde in the presence of 4 equiv each of glacial acetic acid (HOAc) and sodium triacetoxyborohydride [$Na(OAc)_3BH$] in 1,2-dichloroethane (DCE) overnight at room temperature to yield the corresponding bis-benzyl pyrazine **4** (R = Et, $R_1 = CH_2Ph$) in 80% yield. The overall yield of 54% from **1** is clearly superior to <3% realized earlier via base-induced alkylations.[18]

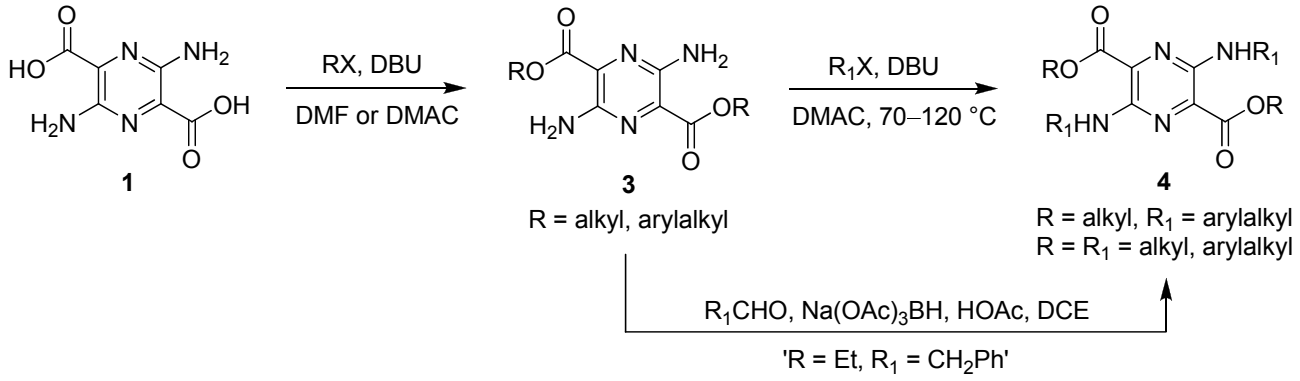

Scheme 1. Alkylation of small molecule aminopyrazines.

Encouraged by these early results, we examined a common intermediate **5a** that was prepared in 78% yield from **1** by standard coupling reaction using EDC-HOBt methodology.[21] Thus, compound **5a** was reductively alkylated with

propionaldehyde in the presence of HOAc and sodium $Na(OAc)_3BH$ in DCE to give **6a** in 80% yield (Scheme 2). No trace of the overalkylated tetra-propyl derivatives were formed in the reaction. The reaction was found to be very clean and robust and the methodology was extended to a variety of aldehydes leading to the corresponding products **6b–6g** in excellent yields (72–95%). Similarly, compound **5b** (79%) that was prepared from **1** and *N*-carbobenzoxy1,2-diaminoethane using EDC-HOBt coupling, was smoothly transformed to **6h** (70%) by treating with Boc-aminoacetaldehdye under reductive amination conditions. The orthogonal protecting groups on the side chains of **6f** and **6g** render the flexibility to conjugate different hydrophilic groups later.

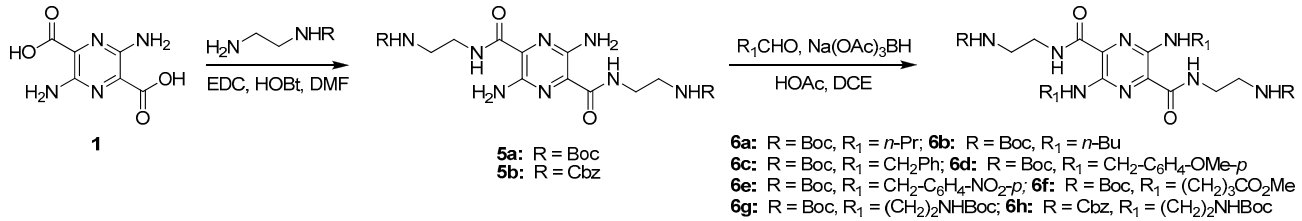

Scheme 2. Synthesis of small molecule pyrazine scaffolds by reductive amination.

The small molecule tetra-substituted pyrazines described above are all lipophilic, but possess handles for further chemical modification to render them hydrophilic. For our current needs, we decided to conjugate PEGs to pendant groups via PEGylation.[22,23] Biodistribution studies of PEG chains upon i.v. administration revealed that the terminal half-life in the circulation increased from 18 min to 1 day as the molecular weight increased from 6,000 to 19,000.[24] The lower molecular weight PEG chains (<6000 Da) are known to be filtered by the glomerulus and not absorbed by renal tubules,[24] and since the terminal half-life of 18 min would be quite acceptable for a renal agent, we decided to utilize activated forms of lower molecular weight methoxy-terminated PEGs[25] for conjugation of the pyrazine scaffold. Thus, the first long wavelength pyrazine-PEG conjugate **8** (42%) was synthesized by initial deprotection of Boc-groups from the intermediate **6a** followed by acylation of the resulting free amine with *N*-hydroxysuccinimide (NHS) ester of 12-mer m-dPEG-acid (**7**) in the presence of 4-methylmorpholine (NMM) and purification by preparative HPLC (Scheme 3).[26] A similar Boc-deprotection of intermediate **6g** followed by reaction with **7** and NHS ester of 24-mer m-dPEG-acid (**9**) gave tetra-PEG conjugates **10a** and **10b** respectively. Compound **10c** containing different size PEG-moieties on the amino- and carboxyl-groups was prepared from orthogonally bis-protected intermediate **6h** by a series of deprotection and conjugation sequences [(i) TFA–CH_2Cl_2, (ii) NMM, NHS ester **7**, (iii) 10% Pd-C, HCO_2NH_4, MeOH–H_2O, and (iv) NMM, NHS ester **9**].

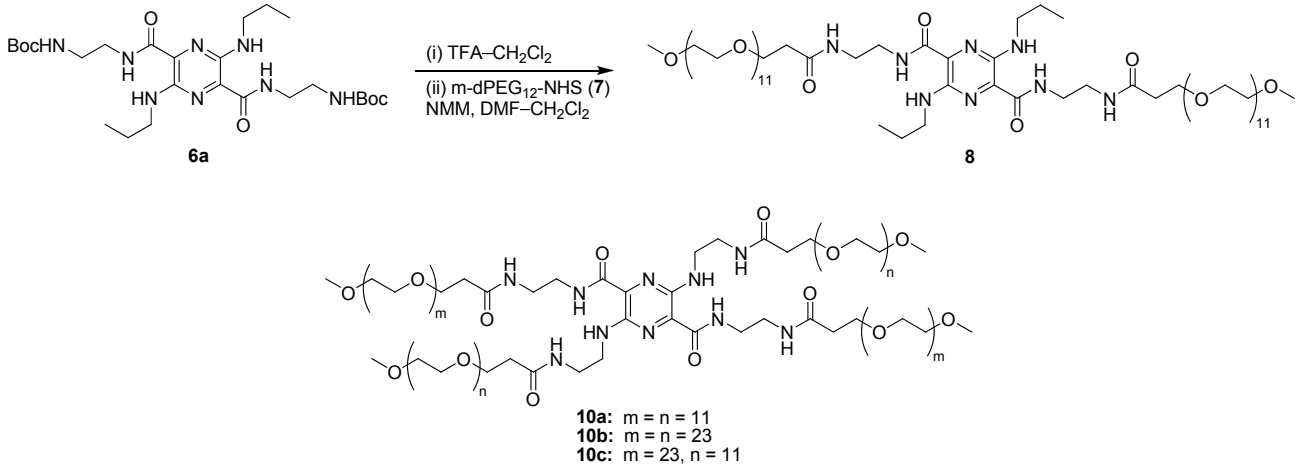

Scheme 3. Synthesis of long wavelength pyrazine-PEG conjugates with diamino spacers.

An alternate class of tetra-PEG conjugates was developed since there are some concerns about plasma stability of the above compounds possessing multiple amide linkages. The diamine spacer was excluded with initial m-dPEG-NH_2 coupled to the carboxyl group and pyrazine amine reductively alkylated later using the appropriate aldehyde (Scheme 4).[27] Standard coupling of **1** with m-dPEG-amines **11a** and **11b** with PyBOP gave the corresponding amides **12a** and **12b** respectively. The crude products were either dialyzed quickly using SpectraPor 7 dialysis tubing (MWCO 1000 or 2000)

or filtered through YMC C18 silica gel to remove excess reagents and the semi-pure compounds were used as such in subsequent reactions. Compound **12a** was alkylated with 3 equiv of appropriate 12-mer m-dPEG-aldehyde in the presence of 3 equiv each of HOAc and sodium $Na(OAc)_3BH$ in DCE to give 1**3a** (68%) and **13b** (61%) respectively. Similarly, several long wavelength analogs **14** and **15a–15g** were synthesized from **12b** by reductive alkylation with propionaldehyde and appropriate m-dPEG-aldehyde respectively.[28]

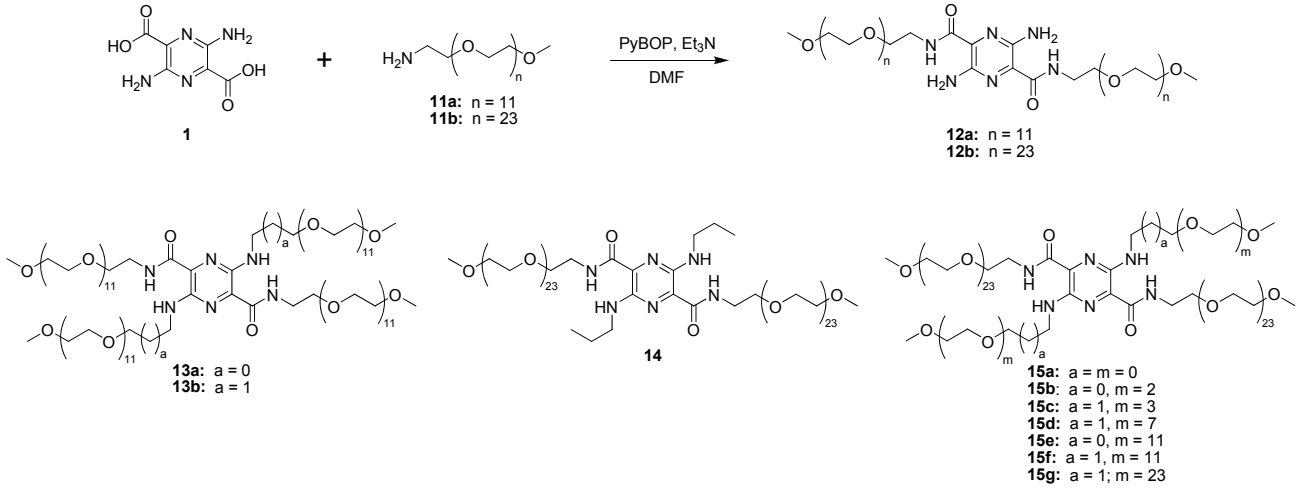

Scheme 4. Synthesis of pyrazine-PEG conjugates without diamino spacers.

2.2. Photophysical properties and protein binding.

In general, each compound was dissolved in PBS buffer to form a 2 mM stock solution. The UV absorbance properties were determined on a 100 μM solution in PBS using a UV-3101PC UV-Vis-NIR Scanning spectrophotometer system from Shimadzu. The fluorescence properties (λ_{ex}, λ_{em}, and CPS at λ_{em}) were determined on a 10 μM solution in PBS using a Fluorolog-3 spectrofluorometer system from Jobin Yvon Horiba. The percent plasma protein binding was determined on a 20 μM compound solution in rat plasma incubated at 37 °C for 1 h. The separation of free from bound was made using an Amicon Centrifree YM-30 device (Regenerated Cellulose 30,000 MWCO) and a Z400K Refrigerated Universal Centrifuge from Hermle. The concentration of protein-free was determined via HPLC analysis using a set of external calibration standards and fluorescence detection.

2.3. Urine elimination studies.

Rat urine elimination studies were conducted in either conscious or anesthetized Sprague-Dawley rats. The test compound (1 mL, 2 mM in PBS) was administered by tail vein injection into conscious, restrained rats, with subsequent collection of urine at the time points of 2, 4 and 6 h post injection. The metabolic cages were washed with water to maximize the recovery of urine discharged at each time point. Alternatively, rats were anesthetized with 100 mg/kg Inactin intraperitoneally, a trachea tube was inserted to maintain adequate respiration, and 1 mL of test compound was injected into the lateral tail vein. Rats were placed on 37 ºC heating pad during the entire experiment. At 6 h post injection, the abdomen was opened, and the urine was removed from the bladder using a 21 gauge needle and a 3 cc syringe. Quantitation of each compound in urine was performed via HPLC analysis using a set of external calibration standards and fluorescence detection. The percent recovery of compound in urine at each time point was calculated based on the balance of mass.

2.4. Non-Invasive optical pharmacokinetic studies.

Male Sprague-Dawley rats (330–380 g) were anesthetized by Inactin (I.P.) or 2% Isoflurane gas anesthesia delivered by a small rodent gas anesthesia machine (RC2, Vetequip, Pleasanton, CA). The animals were placed on a heated board where temperature was maintained between 36–38 ^{o}C. One ear lobe was glued flat to a glass slide positioned approximately 2 mm beneath a fiber optic bundle for recording fluorescence from a test compound passing through the ear. After a 100 second baseline recording, 1 mL of a 2 mM solution was injected into the tail-vein of the rat and the fluorescence signal corresponding to plasma and tissue distribution and subsequent renal clearance of the compound was monitored at the ear. The pharmacokinetic parameters of the compounds were analyzed using WinNonLin pharmacokinetic modeling software (Pharsight, Mountain View, CA) and Microsoft (Redmond, Washington) Excel.

2.5. Optical monitoring apparatus and protocol.

A schematic of the apparatus for non-invasive *in vivo* detection of fluorescence is shown in Figure 1. A nominal 473 nm solid state laser source was employed (Power Technology model LDCU12/7314). The laser source was directed into one leg of a silica bifurcated fiber optic bundle (Oriel #77565). The common end of this bifurcated bundle was placed approximately 2 mm from the rat ear. The second leg of the bifurcated fiber optic bundle was fitted with a collimating beam probe (Oriel #77644). A long pass filter (Semrock LP02-488RS-25) and narrow band interference filter (Semrock FF01-593/40-25) were placed in front of a photomultiplier tube (Hamamatsu photosensor module H7827-011).

A chopper (Stanford Research Systems model SR540) was placed after the laser and before the launch into the bifurcated cable. The output of the photosensor was connected to a lock-in amplifier (Stanford Research Systems model SR830). The lock-in output was digitized (National Instruments NI-USB-6211) and the digitized data was acquired by computer using LabVIEW® data acquisition software.

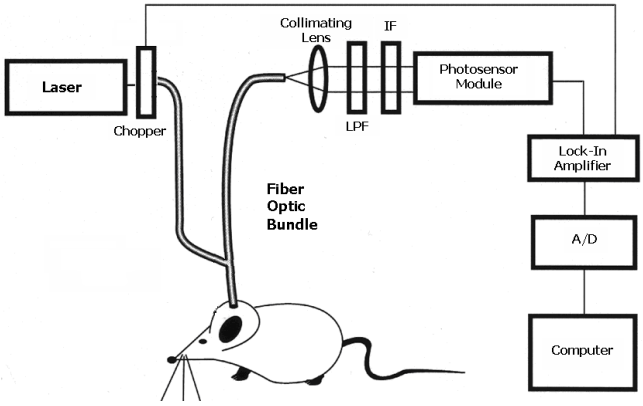

Figure 1. Apparatus for non-invasive in vivo detection of fluorescence.

2.6. Invasive pharmacokinetic studies.

Male Sprague-Dawley rats (330–380 g) were anesthetized by Inactin (I.P.). Rats were surgically instrumented with a trachea tube (PE-190) to facilitate breathing and femoral artery and vein catheters (PE-50 filled with 20 units/mL heparinized saline) for blood sampling and drug administration respectively. After administration of 1 mL of a 2 mM solution of agent, approximately 200 μL blood was sampled and placed into a heparinized tube (Microtainer Brand Tube w/ Lithium Heparin, BD 365971) at 0, 1, 6, 12, 18, 30, 45, 60, 90, 120 min. The concentration of compound in each centrifuged plasma sample was determined via HPLC analysis using a set of external calibration standards and fluorescence detection. The resulting pharmacokinetic parameters of the compound were analyzed using WinNonLin pharmacokinetic modeling software (Pharsight, Mountain View, CA).

2.7. Probenecid inhibition studies.

Six male Sprague-Dawley rats were treated in the same manner as described above in the invasive pharmacokinetic studies. These 6 rats received 70 mg/kg Probenecid (Sigma-Aldrich; St. Louis, MO) 10 min prior to the test compound; this administration was flushed with 0.2 ml NaCl. An additional 6 rats were treated in the same fashion but did not receive probenecid.

3. RESULTS AND DISCUSSION

3.1. Photophysical properties, protein binding, and urine elimination studies.

The linear photophysical measurements of selected small molecule pyrazine compounds were performed in DMSO solutions and are shown in Table 1.[29] All the *N*-alkyl compounds exhibited very similar photophysical patterns, which are significantly enhanced over those of aminopyrazine **5a**. In each of these cases, bathochromic (red) shifts were observed in both the emission and excitation spectra since increased electron donating capabilities of allkylamino groups (donor) results in the enhanced intramolecular charge transfer with the carboxmides (acceptor) in the first excited state. Also, all absorption and excitation spectra are in good agreement with each other, indicating that the observed emission occurs from the main

absorption band. These long wavelength compounds displayed moderate fluorescence quantum efficiences and excited state lifetimes. The rank order of emission quantum yield positively correlates with excited state life time of these compounds.

Table 1. Absorption and fluorescence spectra of small molecule pyrazines **5a**, **6b**, **6d**, and **6g**

compd	absorption λ_{max} (nm)	molar absorptivity (ε)	excitation λ_{max} (nm)	emission λ_{max} (nm)	quantum yield (φ_F)	lifetime τ (ns ± 0.3)
5a	458	12,624	458	548	ND[a]	ND
6b	504	6,806	501	593	0.24	5.49
6d	497	7,599	493	587	0.27	6.59
6g	497	8,219	492	584	0.30	8.55

[a]Not determined.

As an initial screen before biological testing, photophysical properties of all new pyrazine-PEG conjugates and plasma protein binding of most of the compounds were evaluated (Table 2). In addition, urine clearance profiles of the conjugates were determined prior to conducting optical monitoring and invasive pharmacokinetic (PK) experiments. As expected, photophysical properties of all *N*-alkyl compounds are enhanced substantially over those of the bis-amino compound **2a** (λ_{ex} = 449 nm, λ_{em} = 559 nm). In all these cases, bathochromic shifts on the order of 40–50 for excitation and 30–50 for emission were observed, and largest shifts in the emission were found in the case of simple *N*-propyl compounds **8** (λ_{ex} = 498 nm, λ_{em} = 613 nm) and **14** (λ_{ex} = 501 nm, λ_{em} = 611 nm). Among the PEG-conjugates, propionaldehyde based compounds exhibited ~10 nm red shift in the emission spectra over acetaldehyde based compounds (ca. 605 nm for **13b** and 596 nm for **13a**; 602 nm for **15f** and 595 nm for **15e**) and that is in agreement with their relative electron donating capabilities to the pyrazine core.

Table 2. Photophysical properties, urine clearance, and optical monitoring data of pyrazine-PEG conjugates

compd	photophysical properties		urine elimination after 6 h[a] (%)	Optical clearance $T_{1/2}\beta$ [a](min)
	excitation λ_{max} (nm)	emission λ_{max} (nm)		
2a	449	559	86 ± 4 (3)[b]	NA[c]
8	498	613	NA	NA
10a	497	595	101 ± 2 (3)[d]	19.0 ± 0.4 (4)
10b	495	590	NA	NA
10c	495	590	NA	NA
13a	493	596	94 ± 2 (9)	19.4 ± 1.4 (4)
13b	500	605	97 ± 0.4 (3)	19.9 ± 2.4 (3)
14	501	611	85 ± 2 (3)	20.5 ± 2.5 (3)
15a	488	594	NA	NA
15b	490	594	96 ± 1 (3)	16.6 ± 1.3 (4)
15c	494	602	97 ± 2 (3)	14.6 ± 1.1 (4)
15d	498	603	92 ± 4 (3)	19.1 ± 0.8 (4)
15e	495	595	92 ± 1 (3)	18.8 ± 0.8 (4)
15f	499	602	89 ± 2 (3)	20.4 ± 2.0 (4)
15g	495	603	86 ± 7 (3)	17.6 ± 0.9 (4)

[a]Given as mean ± SEM. [b]Numbers in parentheses indicate number of test animals. [c]Not available.
[d]Concious, restrained animals.

The plasma protein binding assay revealed that most of these conjugates show minimal binding to serum proteins (<10%) with >90% unbound material. For example, compound **13a** containing four 12-mer m-dPEG groups with a molecular weight of 2366 Da is essentially free of protein binding (97% unbound). However, compound **14** with a similar molecular weight (2422 Da) containing two 24-mer m-dPEG groups and two hydrophobic *N*-propyl groups show 13% protein binding. Urine elimination studies indicated that all the conjugates showed excellent clearance properties with 85–100% in the urine within 6 h. While 94% of the compound **13a** was present in the urine after 6 h, at that same time point, only 85% of compound **14** was cleared. While presence of hydrophobic groups on the pyrazine amines was found to be detrimental leading to more protein binding and less urine clearance, shielding of the pyrazine core with four PEG-groups certainly helped leading to more clearance. Even though the profile of tetra-PEG conjugate **10a** in all these assays is good for a renal agent (92% protein free, 100% urine elimination), it was found to be less stable than **13a** upon storage in rabbit plasma at various temperatures. HPLC analyses of the samples stored at 0 °C, 4 °C, and −15 °C after 0 d, 7 d, and 35 d indicated that **13a** is far more stable than **10a** for all the storage conditions and duration of storage. While compound **10a** has six amide linkages that are susceptible for proteolytic cleavages whereas **13a** has only two and it is presumed that the number of amide linkages in each molecule might play a role in its stability. Consequently, attention was focused on the compounds of the type **13** and **15** wherein the diamine spacers between the pyrazine core and the conjugated PEGs were eliminated thus decreasing the possibility of proteolytic cleavages.

3.2. Optical monitoring of renal elimination and pharmacokinetic analysis.

Most of the long wavelength compounds were evaluated in animal models for renal function by optical monitoring methods as described in sections **2.4** and **2.5**. All the compounds tested displayed a biphasic elimination profile indicating that they are distributed freely from the blood into the interstitial space and thus conform to at least a two compartment pharmacokinetic model. All the compounds tested displayed very similar optical PK profile with the terminal half-life ($T_{1/2}\beta$) for clearance ranging from 14.6 min to 20.5 min (Table 2, *vide supra*). The elimination profile for compound **13a** (average in 3 animals) monitored by optical methods is shown in the Figure 2a.

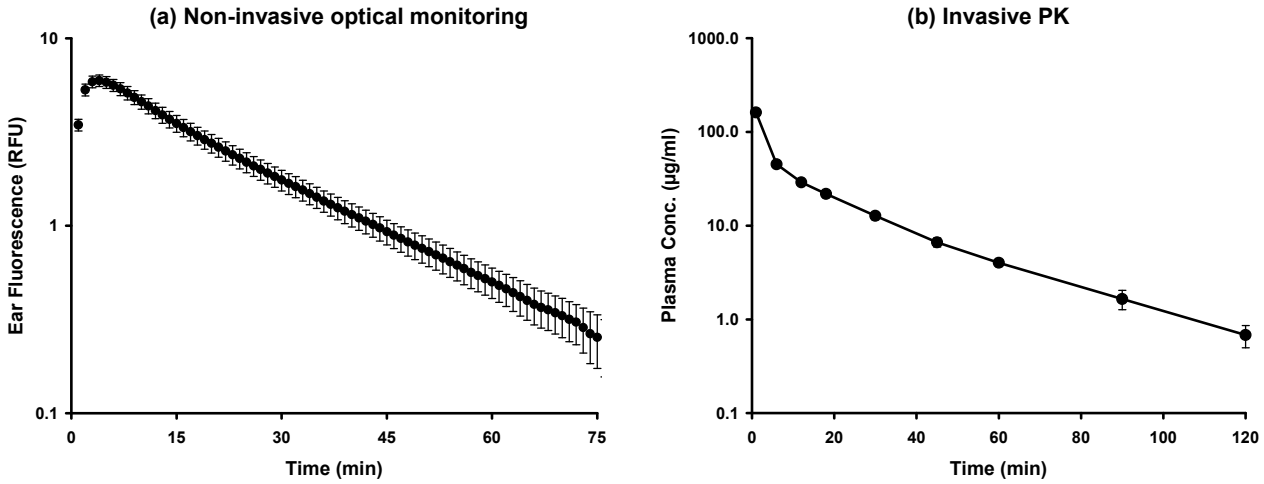

Figure 2. (**a**) Non-invasive optical monitoring and (**b**) invasive PK profile for compound **19a**.

To determine if the ear fluorescence relates to the actual concentration, invasive pharmacokinetic studies were carried out on selected compounds, and the profiles of **10a** and **13a** along with GFR standard iothalamate are presented in Table 3. The elimination profile for compound **13a** (average in 4 animals) is given in the Figure 2b. The tetra-PEG conjugates **10a** and **13a** are comparable to previously described **2b**[15] and iothalamate with regard to clearance indicating that they are indeed GFR agents. The terminal half-life ($T_{1/2}\beta$) for clearance obtained from *in vivo* optical experiment is nearly identical to that derived from invasive plasma PK experiments for both **10a** and **13a**. It should be mentioned here that both these compounds show better urine clearance profiles with >95% excreted at 6 h time point compared to only 80% for iothalamate in our assay. To acertain whether these conjugates clear via glomerular filtration, the rats were first treated with probenicid[30] to inhibit secretion and reabsorption in the renal tubules, and then were administered with **13a**. As can be seen from the comparative clearance rates of **13a** from untreated and probenicid-treated rats, there is virtually no change in its clearance rate indicating the route of elimination exclusively by glomerular filtration.

Table 3. Pharmacokinetic profiles of renal function agents **10a** and **13a**

compd	pharmacokinetics		probenecid (70 mg/kg)	
	clearance $T_{1/2}\beta$ [a] (min)	clearance[a] (mL/min)	clearance $T_{1/2}\beta$ [a] (min)	clearance [a] (mL/min)
2b	21.6 ± 0.6 (3)[b]	2.3 ± 0.0 (3)	NA[c]	NA
10a	18.5 ± 1.0 (3)	2.7 ± 0.1 (3)	NA	NA
13a	19.3 ± 1.0 (9)	3.3 ± 0.1 (9)	23.4 ± 1.8 (6)	3.5 ± 0.1 (6)
Iothalamate	36.6 ± 4.6 (10)	2.7 ± 0.2 (10)	44.1 ± 7.6 (6)	2.0 ± 0.2 (6)

[a]Given as mean ± SEM. [b]Numbers in parentheses indicate number of test animals. [c]Not available.

Time course data from an invasive plasma PK experiment and a non-invasive optical monitoring experiment have been used to correlate *in vivo* fluorescence with plasma concentration. By plotting the average relative fluorescence unit response from three optical monitoring runs versus concentration values from an invasive PK experiment for each time point, an excellent correlation ($R^2 = 0.999$) was demonstrated for the compound **13a** (Figure 3). These results clearly indicate that PK parameters can be determined from the optical clearance data for this class of compounds. Thus, GFR can be estimated with reasonable accuracy from the pharmacokinetic clearance value derived from direct analysis of the non-invasive optical monitoring data.

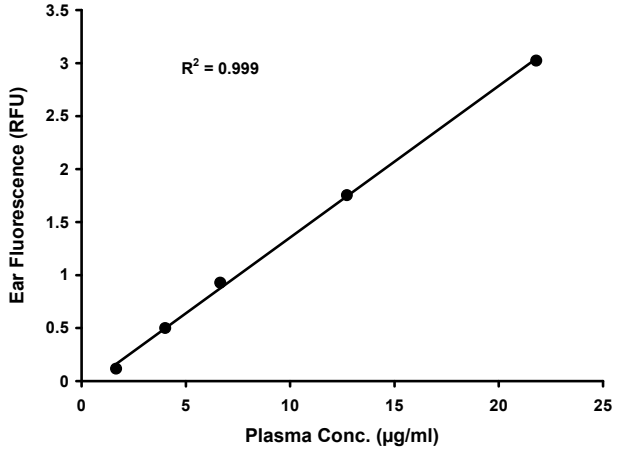

Figure 3. Correlation between optical and plasma pharmacokinetics.

4. CONCLUSIONS

An efficient and proprietary method was developed for the synthesis of N,N'-dialkylated pyrazine analogs exemplified by **6** via reductive amination route. These new pyrazine analogs which absorb and emit at longer wavelengths were utilized as the intermediates for the synthesis of PEG-conjugates of the type **10**. Later the methodology was extended for the synthesis of conjugates **13** and **15** that lack diamine spacers which increases the plasma stability of these compounds. These hydrophilic conjugates were characterized for photophysical properties, plasma protein binding, urine clearance, *in vivo* optical monitoring, and invasive plasma pharmacokinetics. It was demonstrated that the invasive pharmacokinetic profile correlates extremely well with the optical monitoring data and this data could be used to determine renal clearance and hence GFR. The renal clearance properties of some of these conjugates like **10a** and **13a** are either comparable to or superior to the clinical standard iothalamate. Further optimization of pharmcokinetics by continued SAR studies and investigation of toxicological behavior of these long wavelength hydrophilic conjugates of pyrazine will be the focus of future investigations.

Acknowledgement. We thank Dr. Bich Vu for high resolution mass spectra and Dr. Dennis A. Moore for his helpful comments and suggestions in the preparation of this manuscript.

REFERENCES

[1] Dollan, P. D., Alpen, E. L. and Theil, G. B., "A clinical appraisal of the plasma concentration and endogenous clearance of creatinine," Am. J. Med. 32, 65–79 (1962).

[2] Dodge, F.W., Travis, B. L. and Daeschner, C. N., "Comparison of endogenous creatinine clearance with inulin clearance," Am. J. Dis. Child. 113, 683–692 (1967).

[3] Reed, C. H., "Diagnostic applications of cystatin C," Br. J. Biomed. Sci. 57, 323–329 (2000).

[4] Robertshaw, M., Lai, K. and Swaminathan, R., "Prediction of creatinine clearance from plasma creatinine: comparison of five formulae," Br. J. Clin. Pharmacol. 28, 275–280 (1984).

[5] White, C., Akbari, A., Hussain, N., Dinh, L., Filler, G., Lepage, N. and Knoll, G., "Estimating glomerular filtration rate in kidney transplantation: A comparison between serum creatinine and cystatin C-based methods," J. Am. Soc. Nephrol. 16, 3763–3770 (2005).

[6] Sturgeon, C., Sam, A. D. and Law, W. R., "Rapid determination of glomerular filtration rate by single-bolus inulin: a comparison of estimation analyses," J. Appl. Physiol. 84, 2154–2162 (1998).

[7] Wilson, D. M., Bergert, J. M., Larson, T. H. and Leidtke, R. R., "GFR determined by nonradiolabeled iothalamate using capillary electrophoresis," Am. J. Kidney Dis. 39, 646–652 (1997).

[8] Choyke, P. L., Austin, H. A. and Frank, J. A., "Hydrated clearance of gadolinium-DTPA as a measurement of glomerular filtration rate," Kidney int. 41, 1595–1598 (1992).

[9] Lewis, N., Kerr, R. and Van Buren, C., "Comparative evaluation of urographic contrast media, inulin, and ^{99m}Tc-DTPA clearance methods for determination of glomerular filtration rate in clinical transplantation," Transplantation 48, 790–796 (1989).

[10] Dorshow, R. B., Bugaj, J. E., Burleigh, B. D., Duncan, J. R., Johnson, M. A. and Jones, W. B., "Noninvasive fluorescence detection of hepatic and renal function," J. Biomed. Opt. 3, 340–345 (1998).

[11] Rabito, C. A., Chen, Y., Shomacker, K.T. and Modell, M.D., "Optical, real-time measurement of the glomerular filtration rate," Appl. Opt. 44, 5956–5965 (2005).

[12] Yu, W., Sandoval, R. M. and Molitories, B. A., "Rapid determination of renal function using an optical ratiometric imaging approach," Am. J. Physiol. Renal Physiol. 292, F1874–F1880 (2007).

[13] Chinen, L. K., Galen, K. P., Kuan, K. T., Dyszlewski, M. E., Ozaki, H., Sawai, H., Pandurangi, R. S., Jacobs, F. G., Dorshow, R. B. and Rajagopalan, R., "Fluorescence-enhanced europium-diethylenetriaminepentaacetic (DTPA)-monoamide complexes for the assessment of renal function," J. Med. Chem. 51, 957–962 (2008).

[14] Shirai, K., Yanagisawa, A., Takahashi, H., Fukunishi, K. and Matsuoka, M., "Synthesis and fluorescent properties of 2,5-diamino-3,6-dicyanopyrazine dyes," Dyes and Pigments 39, 49–68 (1998).

[15] Dorshow, R. B., Asmelash, B., Chinen, L. K., Debreczeny, M. P., Fitch, R. M., Freskos, J. N.,Galen, K. P.,Gaston, K. R., Marzan, T. A., Poreddy, A. R., Rajagopalan, R., Shieh, J. –J. and Neumann, W. L., "New optical probes for continuous monitoring of renal function," Proc. SPIE, 6867, 68670C-1–68670C-11 (2008).

[16] Weissleder, R. and Ntziachristos, V., "Shedding light onto live molecular targets," Nat. Med. 9, 123–128 (2003).

[17] Taylor, E. C., Jr., Loux, H. M., Falco, E. A. and Hitchings, G. H., "Pyrimidopteridines by oxidative self-condensation of aminopyrimidines," J. Am. Chem. Soc. 77, 2243–2248 (1955).

[18] Kim, J. H., Shin, S. R., Matsuoka, M. and Fukunishi, K., "Self-assembling of aminopyrazine fluorescent dyes and their solid state spectra," Dyes and Pigments 39, 341–357 (1998).

[19] Kim, J. H., Shin, S. R., Matsuoka, M. and Fukunishi, K., "Self-assembling of aminopyrazine fluorescent dyes and their solid state spectra, Part 2," Dyes and Pigments 41, 183–191 (1999).

[20] Abdel-Magid, A. F., Carson, K. G., Harris, B. D., Maryanoff, C. A. and Shah, R. D., "Reductive amination of aldehydes and ketones with sodium triacetoxyborohydride. Studies on direct and indirect reductive amination procedures," J. Org. Chem. 61, 3849–3862 (1996).

[21] Neumann, W. L., Rajagopalan, R. and Dorshow, R. B., "Fluorescent pyrazine derivatives and methods of using the same in assessing renal function," PCT Int. Appl. WO 2007149479 A1 20071227 (2007).

[22] Zalipsky, S., "Functionalized poly (ethylene glycols) for preparation of biologically relevant conjugates," Bioconjugate Chem. 6, 150–165 (1995).

[23] Harris, J. M. and Chess, R. B., "Effect of pegylation on pharmaceuticals," Nature Reviews Drug Discovery 2, 214–221 (2003).

[24] Yamaoka, T., Tabata, Y. and Ikada, Y., "Distribution and tissue uptake of poly (ethylene glycol) with different molecular weights," J. Pharm. Sci. 83, 601–606 (1994).

[25] All PEGylation reagents are discrete, i.e., monodisperse and purchased from Quanta Biodesign, Ltd., Powell, Ohio.

[26] All the pyrazine-PEG conjugates were purified by reverse phase preparative HPLC using a Waters Autopurification system (XBridge™ Prep C18 5 μm OBD™ 30 × 150 mm or Sunfire™ Prep C18 5 μm OBD™ 30 × 150 mm; 0.1% TFA/CH_3CN gradient).

[27] Bentley, M. D., Roberts, M. J. and Harris, J. M., "Reductive amination using poly (ethylene glycol) acetaldehyde hydrate generated in situ: Applications to chitosan and lysozyme," J. Pharm. Sci. 87, 1446–1449 (1998).

[28] m-$dPEG_3$-CH_2CHO was prepared from tri (ethylene glycol) monomethyl ether by Swern oxidation: Carlise, J. R., Kriegel, R. M., Reese, W. S., Jr. and Weck, M., "Synthesis and hydrolysis behavior of side-chain functionalized norbornenes," J. Org. Chem. 70, 5550–5560 (2005).

[29] The linear photophysical properties of compounds **6b**, **6d**, and **6g** were measured by Hyo-Yang Ahn and Professor Kevin D. Belfield at University of Central Florida, Orlando, Florida.

[30] Roch-Ramel, F. and De Broe, M. E., [Renal handling of drugs and xenobiotics. In Clinical Nephrotoxins: Renal Injury from Drugs and Chemicals]; De Broe, M. E., Porter, G. A., Bennett, W. M. and Verpooten, G. A., Eds.; Kluwer Academic Publishers, Dordrecht, 21–46 (2003).